Wind and Structures, *Vol. 29, No. 5 (2019) 313-321*
DOI: https://doi.org/10.12989/was.2019.29.5.313

Numerical modelling of shelter effect of porous wind fences

Prashanth Janardhan*[1] and Harish Narayana[2a]

[1]*Department of Civil Engineering, National Institute of Technology Silchar, Assam, India*
[2]*Department of Civil Engineering, M S Ramaiah Institute of Technology, Bengaluru, Karnataka, India*

(Received November 15, 2018, Revised April 20, 2019, Accepted April 26, 2019)

Abstract. The wind blowing at high velocity in an open storage yard leads to wind erosion and loss of material. Fence structures can be constructed around the periphery of the storage yard to reduce the erosion. The fence will cause turbulence and recirculation behind it which can be utilized to reduce the wind erosion and loss of material. A properly designed fence system will produce lesser turbulence and longer shelter effect. This paper aims to show the applicability of Support Vector Machine (SVM) to predict the recirculation length. A SVM model was built, trained and tested using the experimental data gathered from the literature. The newly developed model is compared with numerical turbulence model, in particular, modified k-ε model along with the experimental results. From the results, it was observed that the SVM model has a better capability in predicting the recirculation length. The SVM model was able to predict the recirculation length at a lesser time as compared to modified k-ε model. All the results are analyzed in terms of statistical measures, such as root mean square error, correlation coefficient, and scatter index. These examinations demonstrate that SVM has a strong potential as a feasible tool for predicting recirculation length.

Keywords: fence; recirculation length; support vector machine; modified k-ε model; CFD simulation

1. Introduction

An open yard in a harbor is subjected to the turbulent wind of high velocity. The presence of vegetation is also low in and around the open yard which leads to high wind erosion. The wind erosion causes the diffusion and drift of lighter stored materials in the open yard. These eroded particles cause various problems viz., reduced visibility, respiratory problems in humans and animals, aesthetic displeasure, and hindering evaporation in plants. Many wind shelter facilities such as obstacles, fences, windbreak forests, halophyte covers, and tillage can be adopted to reduce the drift and diffusion of particles. Several researchers have examined the performance and optimal installation of these facilities to arrest the escaping dust in an open area (Grantz *et al.* 1998, Kim *et al.* 2005, You *et al.* 2006, Dong *et al.* 2007).

The solid and porous fences is one of the methods to prevent wind erosion and provide better shelter in open spaces by reducing the wind velocity in the wake region behind the fence (Perera 1981, Kim *et al.* 2005, You *et al.* 2006, Chen *et al.* 2006, Dong *et al.* 2007, Song *et al.* 2007, Santiago *et al.* 2007, Středová *et al.* 2012, Hong *et al.* 2015, Cheng *et al.* 2016).

The wake, region of recirculation caused by the flow of fluid, generated behind the fence (Fig. 1) is an important application to the environmental problems of turbulent wind interaction between fence and pollutants dispersion. This region traps the pollutants, eroding soil and also helps in preventing material loss. Hence, the fence can be used in controlling erosion problem efficiently and reduce other environmental problems like air pollution. The separated region formed behind the fence determines the reattachment length (i.e. the length of the recirculation zone) which is the single most important length scale, which also describes the flow pattern, with respect to the relative height of the fence. From the separation region to the point of reattachment, the velocity component close to the surface decreases, turbulent flow prevails and substantial pressure gradient exists in the region of reattachment.

The porosity, defined as the ratio of open to the total area of the fence, also affects the flow behind the fence. The flow through the pores increases with increasing porosity thus reducing the low pressure and turbulence behind the fence and also increasing the protected area behind the fence. By varying the porosity of the fence different wind flow patterns and areas of protection can be established. The porous fence causes complex airflow due to the bleed flow through the pores in the fence and the displaced flow passing over the fence. The flow path behind porous fences for porosities above and under critical porosity is shown in Fig. 2. Critical Porosity (P_{crit}) is defined as the maximum fence porosity below which flow separation and reversal occurs. Porosity above critical porosity leads to dominant flow behind the fence with no flow separation and porosity below critical value leads to reversal of flow behind the fence resulting in a region of recirculation. In general, 0.20-0.50 porosity of the fence provides noticeable changes in flow circulation behind the fences (Jensen 1954, Tani 1958, Raine and Stevenson 1977). The low recirculating wind created in the recirculation region behind the porous wind fence traps the eroded particles and controls the material loss.

*Corresponding author, Assistant Professor
E-mail: prashnitk.hsn@gmail.com
[a] Associate Professor

http://www.techno-press.com/journals/was&subpage=7 ISSN: 1226-6116 (Print), 1598-6225 (Online)

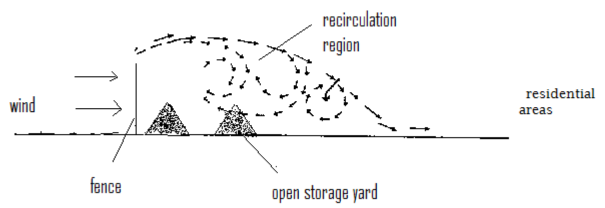

Fig. 1 Pollution control from open storage yard using the fence

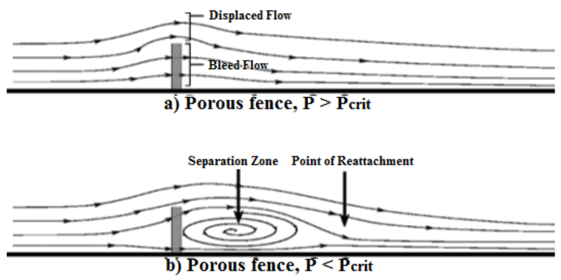

Fig. 2 Comparison of flow path behind porous fences (Xu and Mustafa 2015)

In recent years, many investigators focused on the efficacy of fences by evaluating the reduction in wind velocity in the wake region behind the fence. There are numerous experimental studies and numerical simulations to study the shelter effect of porous fences. The aerodynamics of wind fences mainly depends on mean velocity and turbulence intensity which are often given as justification for evaluating the shelter effect of the fence (Hagen 1976, Dong *et al.* 2010). For a porous fence farm (series of fences placed parallel to each other) the fence characteristics like the height of fence, porosity, the distance between neighboring fences and porosity distribution influences the wind velocity reduction and turbulence features (Cornelis and Gabriels 2005, Ferreira 2011).

However, for an isolated porous wind fence, the most crucial parameter is the porosity which influences the performance of shelter devices (Grantz *et al.* 1998, Song *et al.* 2007). Porous fence with 20% porosity showed better reduction in leeward mean velocity (Raine and Stevenson 1977). The experiments on porous fence showcased that 40% porosity with an optimum fence space to height ratio (bottom gap ratio) between 6 to 8 reduced the wind damage in the wake region (Papesch 1992). Numerical simulations with porous fences with porosity less than 29.9% would have recirculation region behind the fence and porosity of 10.2% gave optimum shelter effect (San *et al.* 2018). The porous fence of porosity 40% was effective for decreasing the mean pressure and pressure fluctuation in and around the coal piles (Lee and Park 2000). The flow behind a porous fence with a bottom gap of 0.1 gives a good shelter effect similar to that of the no-gap fence in the large wake region behind the fence (Kim and Lee 2002). The study comparing different k-ε models recommended RNG k-ε model for computation of indoor air flow (Chen 1995). Numerical simulation studies using RANS equations with the standard k-ε model found that 30% porous wind fence seemed most effective in reducing the dust emission (Chen *et al.* 2012). The modified realizable k-ε model performed better than standard k-ε model in simulating axisymmetric turbulent buoyant plume (Van Maele and Merci 2006). The experimental and numerical studies on solid and porous wind fences with different bottom gap ratios showed that the bottom gap ratio of 0.1 with a porosity of 10% was effective in holding the dust particles in the wake region and modified k-ε model produced better results than eight other turbulence models considered in the study (Janardhan *et al.* 2011). Various forms of the k-ε model turbulent model were tested and found the realizable k-ε model simulated the field conditions effectively (Bourdin and Wilson 2008). Neural network approach was successfully adopted to predict wind speed-up over terrain features, specifically, isolated hills, double hills, and triple hills (Bitsuamlak *et al.* 2006).

Although the experts have made better improvement in analyzing the effect of porosity through experimental and numerical studies, there are no definite guidelines on the shelter performance of the porous fences. The existing CFD, on-site wind measurement and wind tunnel simulations are complicated, time consuming and labor-intensive. Thus, the primary objective of this research is to develop a new method which is easy to use and cost effective with improved prediction accuracy. In the present research, it was chosen to adopt an empirical approach and the neural network specifically Support Vector Machine (SVM) based approach was found promising. This approach has high accuracy and easy to implement. By using SVM better generalization can be achieved. SVM adopts structural risk minimization principle which rather than minimizing the error on training data only it minimizes the bound on the generalization error of the model. It has better generalization capability and avoids overtraining as compared to Artificial Neural Networks (ANN) model. Also, SVM outperforms ANN in terms of accuracy and stability and therefore it is a viable alternative in cases where there is very little margin for error. Further, as and when new data is available, better results can be achieved by presenting new training examples to SVM. Hence, in this present paper, the performance of SVM technique in predicting reattachment length is investigated.

2. Methodology

2.1 Experimental data

The data was obtained from Janardhan *et al.* (2011) from the experiments carried out at National Institute of Technology (NITK), Surathkal, India. The wind tunnel used for the experiments was a low-speed wind tunnel. The test section is rectangular in shape with the cross-sectional area of 0.61 m X 0.61 m and total length is 1.2 m. Fig. 3 shows the sketch of wind tunnel. Transparent windows are provided on both sides of the test section to enable proper visualization of the model. Standard Pitot-static tube was used for pressure measurement.

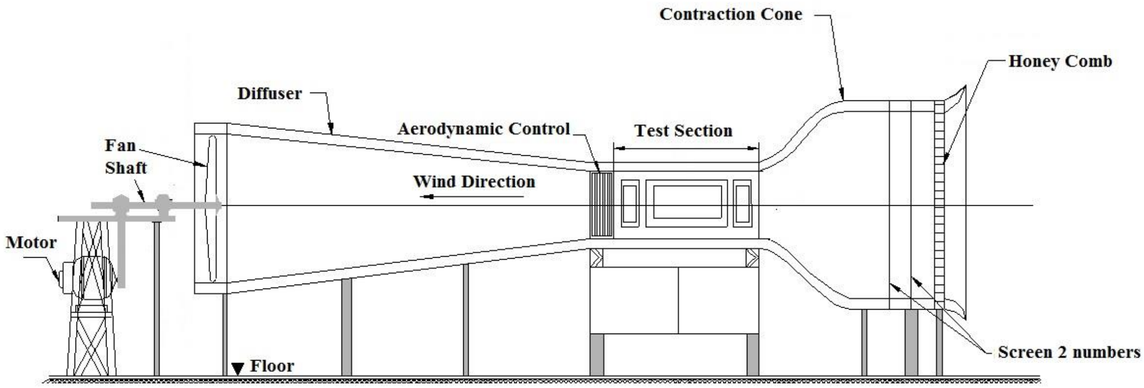

Fig. 3 General layout of the low speed wind tunnel facility at NITK, Surathkal

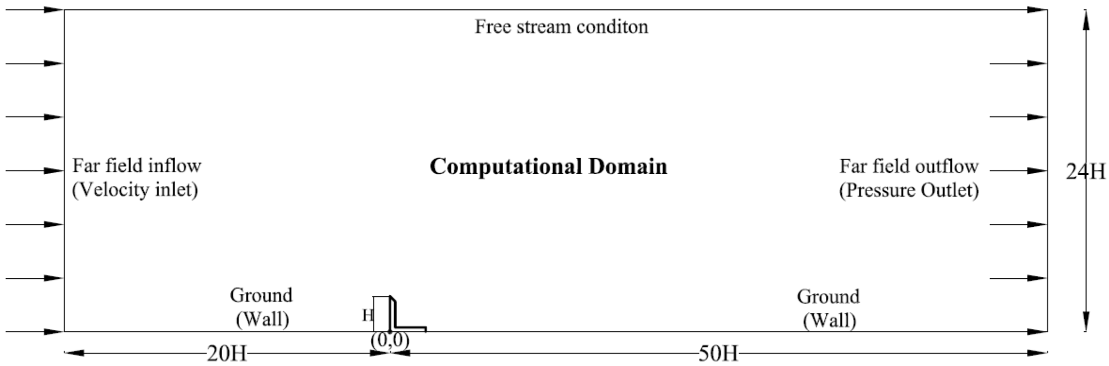

Fig. 4 Defining the computational domain

Table 1 Range of experimental variables

Variable	Range of values
Porosity (P)	0, 10%, 20%
Gap ratios (G/H)	0, 0.1, 0.2, 0.3
Free stream velocity (v) m/s	7.5, 10, 12.5

The experiments were conducted with three different porosities placed at varying gap ratios. The fence height (H) was 0.0254 m and thickness (B) was 0.003 m. The material used for the fence is stainless steel. Three free stream velocities were considered for the experimental study. The geometric values were made dimensionless by the height of the fence ‘H’. One of the main advantages is the predictions would be independent of scale and Reynolds number (R_e), which is an essential assumption when applying wind tunnel results to a full-scale case. The experimental variables considered for the experiment are shown in Table 1.

2.2 Numerical simulation procedure

A numerical two-dimensional flow field analysis was performed. Turbulent and incompressible flow was assumed. The CFD analysis was done by using the software ANSYS Multiphysics. The two-dimensional computational domain chosen is shown in Fig. 4. The accuracy of the CFD solution is mainly dependent on the boundary conditions imposed on the computational domain. The upper and ground surface is considered as wall surfaces. On wall surfaces, the normal component of velocity is set to zero, since, no fluid can pass through the wall.

In addition, the tangential component of velocity at a stationary wall is set to zero because of the no-slip condition. All the variables (horizontal and vertical components of velocity) are set to zero at the ground and the pressure is set to zero at the outlet boundary. Different inlet velocities considered for the present study were 7.5, 10 and 12.5 m/s. At the velocity inlet, these velocities were specified along the inlet edge. Pressure at velocity inlet and velocity at pressure outlet are not specified at as this would lead to mathematical over specification. Rather, these parameters adjust itself to match the rest of the flow field.

The character of the flow is to be estimated i.e., whether the flow is laminar or turbulent. The parameter used to calculate the flow regime is called the Reynolds number. This character is a function of the fluid properties, geometry, and the approximate magnitude of the velocity field. Reynolds number is calculated by using the formula

$$R_e = \frac{\rho V L_c}{\mu} \tag{1}$$

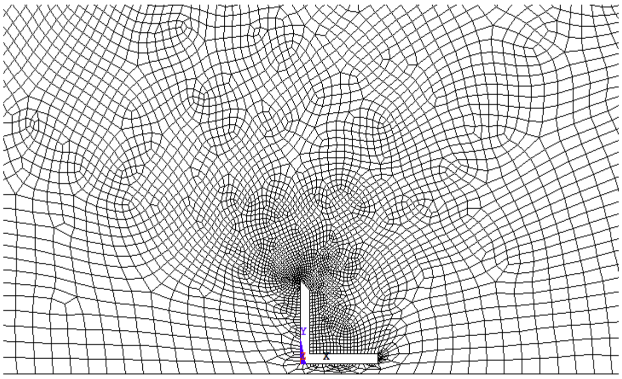

Fig. 5 Computational domain with non-orthogonal grid system

Where
ρ= Density of air, 1.204 kg/m^3
V = Velocity of air, m/s
L_c = Characteristic length of the geometry in m i.e., the height of fence
μ = Dynamic viscosity of air, 1.825x10^{-5} kg/m.s

In the present study, turbulent flow over fences was assumed. Hence, the Reynolds number based on the fence heights and wind velocities ranges from 1.257x10^4 to 2.094x10^4. The wind flow over the fence is assumed to be incompressible.

In the case of CFD using turbulence models all the unsteady turbulent eddies are solved with the use of a turbulence model. Mathematical models are employed to take into account the enhanced mixing and diffusion caused by turbulent eddies. For simplicity, only steady, incompressible flow is considered. When using a turbulence model, the steady Navier-Stokes equation is replaced by the Reynolds Averaged Navier-Stokes (RANS) equation.

$$\left(\vec{V}.\vec{V}\right)\vec{V} = -\frac{1}{\rho}\vec{V} + \vartheta\nabla^2\vec{V} + \vec{V}\left(\tau_{ij,turbulence}\right) \quad (2)$$

Where $\tau_{ij,turbulence}$ is known as the specific Reynolds stress tensor which contains 6 variables. These unknowns are modelled in various ways by turbulence models. In order to check the suitability of the turbulence models, different models were chosen and the study was conducted on one of the porous fence for a gap ratio of 0 with a wind speed of 10 m/s. Modified k- ε model (Packwood 2000) suited well for our test conditions which slightly underestimated the recirculation region but compared to other models the length was agreeable with the experimental results. Similar work with different turbulence models and same modified k- ε model was found agreeable (Kim and Lee 2002, Bourdin and Wilson 2008, Packwood 2000, Purthviraj *et al.* 2011).

The mesh generated for numerical analysis is non-orthogonal mesh system (unstructured quadrilateral grids) with higher nodal density along the ground and upper surface in order to attain higher resolution. Fig. 5 shows the mesh details near and far from the fence. The mesh density is enhanced around the fence and along the bottom surface of the flow domain. Various mesh sizes were tested on one of the porous fence for a gap ratio of 0 with a wind speed of 10 m/s to get grid independent results. The grid independence was observed for a mesh size of about 583735 elements. Similarly, for different fence models the number of elements ranged from 168020 to 583735.

2.3 Support Vector Machine (SVM)

SVMs are powerful statistical learning artificial algorithms used for classification or regression (Samui 2008, Burges 1998, Cristianini and Shawe-Taylor 2000, Vapnik 1998, Vapnik 1999). It has been successfully applied in the field of hydrology (Chen and Yu 2007), construction engineering (Ni *et al.* 2005), image recognition (Yang *et al.* 2002), ocean modelling (Harish *et al.* 2015, Mandal *et al.* 2012) and many more fields. The basic idea of the SVM is to map the input space into a high-dimensional by non-linear transformation. The SVM is capable of generalizing and resolving problems involving small samples, non-linearity and high-dimensional input space (Kecman 2001).

A brief description about Support Vector Regression (SVR) theory is given. The alternative loss function are introduced to solve the regression problems by SVM. The regression model can be linear or non-linear. Linear models consist of three loss functions viz., Huber, quadratic and e-intensive loss functions. For non-linear models, the data must be mapped to higher dimensional space where linear regression is performed. The kernel approach is utilized to address the dimensionality issue. It is essential to know about the problem and the distribution of noise in SVR modelling. Huber loss function is a good alternative in the absence of such knowledge (Cristianini and Shawe-Taylor 2000, Cortes and Vapnik 1995).

Consider a set of training samples $\{xi, yi\}$, i = 1, 2, . . . n, $xi \in R^d$, $yi \in R$, where xi is an input vector, yi is the corresponding output value, and n is the number of training samples. The regression problem is to choose a function that predicts the real estimation of y as nearly as could be expected, with a precision of ε. Therefore, the purpose of the SVM is to seek the optimum regression function

$$f(x) = wx + b \quad (3)$$

where, $\omega \in R^n$ and $b \in R$, ω is an adjustable weight vector, b is the scalar threshold; Rn is n-dimensional vector space, and x is one-dimensional vector space.

It is clear from the statistical theory that the regression function is determined by the minimization of the objective function in SVM. The parameters of the regression function (ω and b) are evaluated by minimizing the regularized risk function as follows:

Minimize

$$\frac{1}{2}||\omega||^2 + C\sum_{i=1}^{n}(\xi_i + \xi_i^*) \quad (4)$$

Subject to

Table 2 Different kernel functions

Kernels	Functions
Polynomial	$K(x_i,x_j) = [(x_i.x_j)+1]^d, \quad d = 1,2,\dots.n$
rbf	$K(x_i,x_j) = exp\left\{-\|x_i - x_j\|^2/2\sigma^2\right\}$
erbf	$K(x_i,x_j) = exp\left\{-\|x_i - x_j\|/2\sigma^2\right\}$
spline	$K(x_i,x_j) = 1 + x_i x_j + x_i x_j\, min(x_i,x_j) - \frac{x_i + x_j}{2}(\min(x_i,x_j))^2 + \frac{1}{3}(\min(x_i,x_j))^3$
b-spline	$K(x_i,x_j) = B_{2n+1}(x_i - x_j)$

$$y_i - [(\omega \cdot x_i) + b] \le \varepsilon + \xi_i$$
$$[(\omega.x_i) + b] - y_i \le \varepsilon + \xi_i^* \tag{5}$$
$$\xi_i \ge 0, \xi_i^* \ge 0, i = 1,2,\dots.$$

where C>0 is a penalty factor, ξ and $\xi*$ are slack variables. ε is the insensitive loss function and can be described in the following way

$$L_\varepsilon(y) = f(x) = \begin{cases} |f(x) - y| - \varepsilon, & |y - f(x)| \ge \varepsilon \\ 0, & otherwise \end{cases} \tag{6}$$

The dual optimization problem can be further presented by utilizing Lagrangian multipliers and maximizing the objective function.

Maximize:

$$\sum_{i=1}^{n} y_i(\alpha_i^* - \alpha_i) - \varepsilon\sum_{i=1}^{n}(\alpha_i^* + \alpha_i) - \frac{1}{2}\sum_{i=1}^{n}\sum_{i=1}^{n}(\alpha_i^* - \alpha_i)(\alpha_j^* - \alpha_j)(x_i,x_j) \tag{7}$$

Subject to

$$\sum_{i=1}^{n}\alpha_i = \sum_{i=1}^{n}\alpha_i^*, \qquad 0 \le \alpha_i^* \le c, \;\; 0 \le \alpha_i \le c \tag{8}$$

where the α_i, α^*_i are called Lagrangian multipliers. The samples with non-zero Lagrangian multipliers are called as support vectors and if the multipliers are equal to zero then the training object will become irrelevant to the final solution.

The input data must be mapped into higher dimension space using non-linear mapping functions when linear regression is not fitting into the dataset. A non-linear transformation (x) replaces the input x in (7), and the regression function can be written as

$$f(x) = \sum_{i=1}^{nsv}(\alpha_i - \alpha_i^*)k(x_i,x_j) + b \tag{9}$$

where nsv is the number of support vectors and $k(x_i,x_j) = \phi(x_i)\cdot\phi(x_j)$, $k(x_i,x_j)$ is a kernel function. Kernel functions can be selected based on Merce's condition (Vapnik *et al.* 1996, Vapnik 2013). Some of the kernel functions used in the present study are tabulated in Table 2 (Gunn 1998).

2.3.1 SVM for predicting the recirculation length

As mentioned previously, there are numerical and experimental methods to determine the recirculation length behind a fence. This study attempts to utilize SVM for the prediction of recirculation length. For the present study, experimental data are divided into 75% training set and 25% testing set.

In the case of SVM training, five types of kernel functions were used, namely, radial bias function (rbf), exponential radial basis function (erbf), spline, b-spline and a polynomial function. The kernel specific parameters during the training process are chosen by trial and error approach. The optimal parameters of different kernel functions of SVM are briefed in Table 3. In rbf and erbf kernel, the optimal width (γ) obtained are 1 and 3 respectively. The obtained optimal values of d (degree) for both polynomial and b-spline kernel function is 1. It is found that nsv is 100% for all SVM models, which indicates that there is no noise in the data set.

The capability of the approach is determined using statistical measures namely Correlation Coefficient (CC), Root Mean Square Error (RMSE) and Scatter Index (SI), which are defined as

$$CC = \frac{\sum_{i=1}^{n}(O_i - \bar{O}_i)(P_i - \bar{P}_i)}{\sqrt{\sum_{i=1}^{n}(O_i - \bar{O}_i)^2(P_i - \bar{P}_i)^2}} \tag{10}$$

$$RMSE = \sqrt{\frac{1}{n}\sum_{i=1}^{n}(O_i - P_i)^2} \times 100\% \tag{11}$$

$$SI = \frac{RMSE}{\bar{O}_i} \tag{12}$$

Where, O_i and P_i are the observed and predicted recirculation length respectively, n is the number of data set used and $\bar{O}_i$ and $\bar{P}_i$ are average observed and predicted recirculation length respectively.

3. Results and discussions

The comparison between experimental and numerical values of recirculation length can be seen in Fig. 6. It is

Table 3 Optimal parameters for SVM models with different kernel functions

Kernel	nsv	C	ε	γ	d
Polynomial	27	3	0.0012	-	1
rbf	27	1000	0.0003	1	-
erbf	27	1500	0.0002	3	-
spline	27	300	0.0015	-	-
b-spline	27	10	0.0012	-	1

Table 4 Optimal parameters for SVM models with different kernel functions

	Training			Testing			Numerical simulation		
Kernel	CC	RMSE	SI	CC	RMSE	SI	CC	RMSE	SI
b-spline	0.9946	0.3383	0.0314	0.9529	0.8624	0.0755			
spline	0.9999	0.0478	0.0044	0.9220	1.3780	0.1206			
erbf	0.9999	0.0646	0.0060	0.9470	1.0398	0.0910	0.993	1.663	0.152
Poly	0.9045	1.6832	0.1561	0.8974	1.5720	0.1376			
rbf	0.9807	0.6436	0.0597	0.9279	1.0726	0.0936			

evident from the graph that the modified k-ε turbulence model performs better with a R^2 of 0.9801. The non-orthogonal grid is more preferable in a modified k-ε model for predicting the flow field. The modified k-ε model tends to slightly overestimate the prediction. The modifications in the model tries to solve some standard k-ε problems like violation of Schwartz inequality for shear stress where there are large strain rates (Santiago *et al.* 2007). The experimental measurements very near to the fence is not available. Hence, the validity of the modified k-ε model cannot be tested near the fence and the results obtained from the numerical study has to be verified carefully. The Shelter effect was high for low porosity fence (Sagrado *et al.* 2002, San *et al.* 2018). In general, the alterations for the adverse pressure gradient flows improved the prediction in the modified k-ε turbulence model.

The performance of predicting the recirculation length using SVM and numerical model is assessed in terms of statistical measures as shown in Table 4. All kernels showed good correlation between the observed and predicted recirculation length with CC more than 0.9045 and 0.8974 for training and testing respectively. By comparing all the kernels it was observed that the b-spline kernel shows good performance with CC more than 0.9946 and 0.9529, RMSE less than 0.3383 and 0.8624, SI with 0.0314 and 0.0755 for training and testing respectively. The comparison of experimental and SVM model for training and testing dataset is shown in Fig. 7.

All models were run in DELL INSPIRON with Intel®coreTMi5 CPU@2.67 GHz, 4 GB RAM and 64 bit windows 7 operating system. The numerical model took 10 hours to solve one configuration of fence with a single velocity and gap ratio. The SVM model took about less than a minute to model the complete dataset. From the comparison between the b-spline kernel SVM and numerical models it is clear that the numerical model has a better prediction capability with a CC of 0.993. But, the RMSE and SI are higher as compared to the b-spline kernel SVM model. Even though the prediction is better with a numerical model, the computation time required is very high than the SVM model. Thus, the SVM model with b-spline kernel can be considered as an alternative to the numerical model when time is a constraint and when lower RMSE and SI are required. Furthermore, the SVM model has good generalization capacity to avoid overtraining, and can always be updated to get better results by presenting new training examples as new data become available. Thus, the SVM model can be regarded as a very effective method to predict the recirculation length behind a porous wind fence.

For convenient comparison, the experimental and predicted results from both the models are plotted in Fig. 8. It can be seen that the results from the SVM method are in good agreement with the experimental results. The SVM model with b-spline kernel function has shown a similar pattern compared to experimental data. Further, the prediction by the modified k-ε model is slightly overestimated than the experimental results.

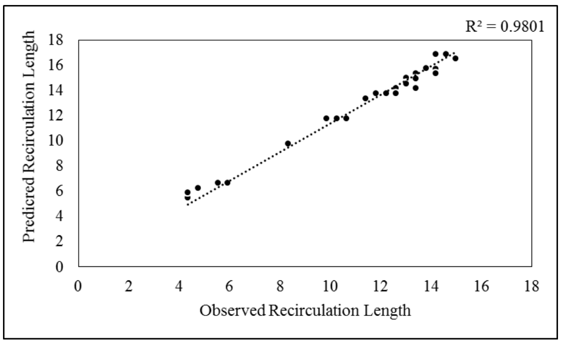

Fig. 6 Comparison of experimental and numerical values

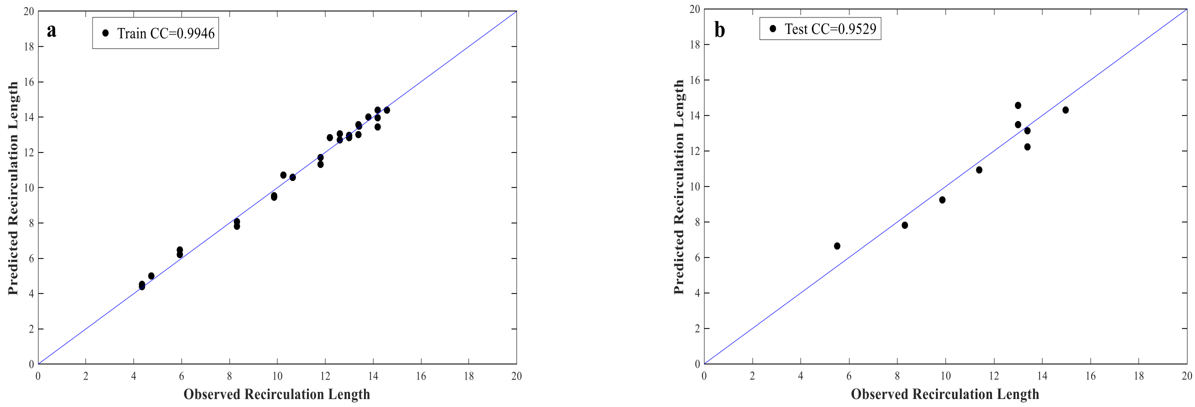

(a) Training CC (b) Testing CC

Fig. 7 Observed and predicted recirculation length (b-spline)

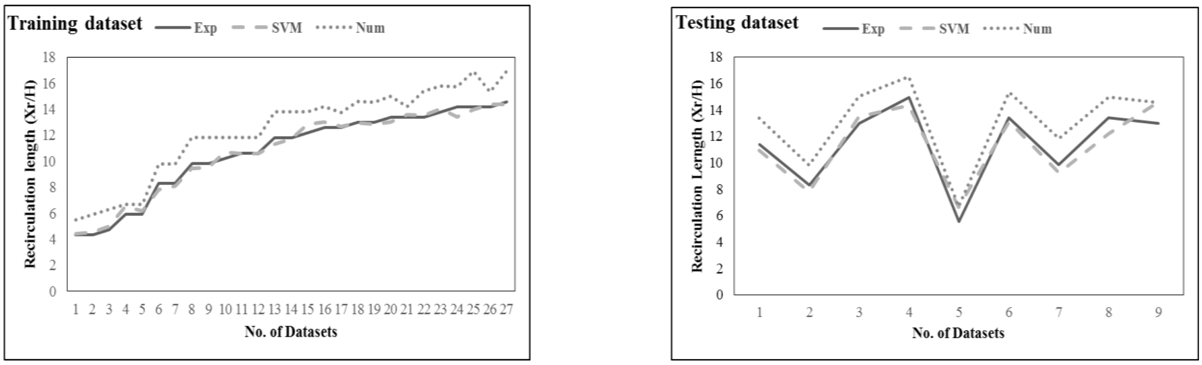

(a) Training dataset (b) Testing dataset

Fig. 8 Comparison of experimental results to results of SVM and numerical analysis.

4. Conclusions

This present study reports a new and influential approach for predicting the recirculation length using SVM for the first time in the literature. After learning from a set of selected training data, involving porosity, gap ratio and velocity collected from the previous literature, the SVM can be utilized to predict the recirculation length behind the fence.

The SVM modelling is primarily driven by the appropriate selection of the kernel function for satisfactory results. In this paper, few kernel functions are compared and it is found that b-spline is better able to predict the recirculation length with an acceptable degree of accuracy.

The comparison of experimental with b-spline kernel SVM and numerical model showed that the even though the numerical model predicted the recirculation length with high CC the RMSE and SI was also high compared to the SVM model. Further, taking into consideration the time for solving the problem it is clearly evident that SVM can predict the recirculation length with good accuracy in lesser time.

The statistical parameters of RMSE, and R^2 show that the proposed SVM model results have the best accuracy and can predict recirculation length very close to experiment results. The use of SVM is very advantageous for the prediction of the recirculation length because it can perform non-linear regression efficiently for high-dimensional data sets. Furthermore, its solution is global. The satisfactory predictions of the recirculation length by the model indicate that SVM is a useful modelling tool for engineers and research scientists at solving complex flow fields. Lastly, although SVM model could be used as an alternative tool to predict recirculation length, it requires experimental data for changing flow fields and configuration of the test model. Also, CFD simulations can be a good comparative tool with the developed numerical model.

Acknowledgments

The authors would like to thank the Director of National Institute of Technology Silchar and Principal of Ramiah Institute of Technology for their support to carry out the work.

References

Bitsuamlak, G., Stathopoulos, T. and Bédard, C. (2006), "Effects of upstream two-dimensional hills on design wind loads: a computational approach", *Wind Struct.*, **9**(1), 37-58. http://dx.doi.org/10.12989/was.2006.9.1.037.

Bourdin, P. and Wilson, J.D. (2008), "Windbreak aerodynamics: is computational fluid dynamics reliable?", *Bound.-Lay. Meteorol.*, **126**(2), 181-208. https://doi.org/10.1007/s10546-007-9229-y.

Burges, C.J. (1998), "A tutorial on support vector machines for pattern recognition", *Data Min. Knowl. Disc.*, **2**(2), 121-167. https://doi.org/10.1023/A:1009715923555.

Chen, G., Wang, W., Sun, C. and Li, J. (2012), "3D numerical simulation of wind flow behind a new porous fence", *Powder Technol.*, **230**, 118-126. https://doi.org/10.1016/j.powtec.2012.07.017.

Chen, K., Zhu, F. and Niu, Z. (2006), "Evaluation on shelter effect of porous windbreak fence through wind tunnel test", *Acta Scientiarum Naturalium-Universitatis Pekinensis*, **42**(5), 636.

Chen, Q. (1995), "Comparison of different k-ε models for indoor air flow computations", *Numer. Heat Tr. Part B Fund.*, **28**(3), 353-369. https://doi.org/10.1080/10407799508928838.

Chen, S.T. and Yu, P.S. (2007), "Pruning of support vector networks on flood forecasting", *J. Hydrology*, **347**(1-2), 67-78. https://doi.org/10.1016/j.jhydrol.2007.08.029.

Cheng, J.J., Lei, J.Q., Li, S.Y. and Wang, H.F. (2016), "Effect of hanging-type sand fence on characteristics of wind-sand flow fields", *Wind Struct.*, **22**(5), 555-571. https://doi.org/10.12989/was.2016.22.5.555.

Cornelis, W.M. and Gabriels, D. (2005), "Optimal windbreak design for wind-erosion control", *J. Arid Environ.*, **61**(2), 315-332. https://doi.org/10.1016/j.jaridenv.2004.10.005.

Cortes, C. and Vapnik, V. (1995), "Support-vector networks", *Machine Learning*, **20**(3), 273-297. https://doi.org/10.1007/BF00994018.

Cristianini, N. and Shawe-Taylor, J. (2000), "An Introduction to Support Vector Machines and Other Kernel-Based Learning Methods", Cambridge university press.

Dong, Z., Luo, W., Qian, G. and Wang, H. (2007), "A wind tunnel simulation of the mean velocity fields behind upright porous fences", *Agricultural Forest Meteorol.*, **146**(1-2), 82-93. https://doi.org/10.1016/j.agrformet.2007.05.009.

Dong, Z., Luo, W., Qian, G., Lu, P. and Wang, H. (2010), "A wind tunnel simulation of the turbulence fields behind upright porous wind fences", *J. Arid Environ.*, **74**(2), 193-207. https://doi.org/10.1016/j.jaridenv.2009.03.015.

Ferreira, A.D. (2011), "Structural design of a natural windbreak using computational and experimental modeling", *Environ. Fluid Mech,*, **11**(5), 517-530. https://doi.org/10.1007/s10652-010-9203-y.

Grantz, D., Vaughn, D., Farber, R., Kim, B.O.N.G., VanCuren, T. and Campbell, R. (1998), "Wind barriers offer short-term solution to fugitive dust", *California Agriculture,* **52**(4), 14-18. https://doi.org/10.3733/ca.v052n04p14.

Gunn, S.R. (1998), "Support vector machines for classification and regression", *ISIS Technical Report*, **14**(1), 5-16.

Hagen, L.J. (1976), "Windbreak design for optimum wind erosion control," *Publ Great Plains Agric Counc*.

Harish, N., Mandal, S., Rao, S. and Patil, S.G. (2015), "Particle Swarm Optimization based support vector machine for damage level prediction of non-reshaped berm breakwater", *Appl. Soft Comput.*, **27**, 313-321. https://doi.org/10.1016/j.asoc.2014.10.041.

Hong, S.W., Lee, I.B. and Seo, I.H. (2015), "Modelling and predicting wind velocity patterns for windbreak fence design", *J. Wind Eng. Ind. Aerod.*, **142**, 53-64. https://doi.org/10.1016/j.jweia.2015.03.007.

Janardhan, P., Pruthviraj, U. and Subhash, C.Y., (2011), "Shelter Effect of Porous Wind Fences in Open Coal Storage Yard at Harbour", LAP Lambert Academic Publishing. India.

Jensen, M. (1954), "Shelter Effect: Investigations into Aerodynamics of Shelter and its Effects on Climate and Crops, The Danish Technical Press, Copenhagen.

Kecman, V. (2001), "Learning and Soft Computing: Support Vector Machines, Neural Networks, and Fuzzy Logic Models", MIT press, Cambridge, MA, USA.

Kim, H.B. and Lee, S.J. (2002), "The structure of turbulent shear flow around a two-dimensional porous fence having a bottom gap", *J. Fluid. Struct.*, **16**(3), 317-329. https://doi.org/10.1006/jfls.2001.0423.

Kim, H.G., Kim, M.K., Kim, B.E. and Yoon, H.Y. (2005), "Optimization of fugitive dust control system for weather conditions", *Research Institute of Industrial Science & Technology*, **19**(1), 21-31.

Lee, S.J. and Park, C.W. (2000), "The shelter effect of porous wind fences on coal piles in POSCO open storage yard", *J. Wind Eng. Ind. Aerod.*, **84**(1), 101-118. https://doi.org/10.1016/S0167-6105(99)00046-X.

Mandal, S., Subba Rao, Harish, N. and Lokesha (2012), "Damage level prediction of non-reshaped berm breakwater using ANN, SVM, and ANFIS models," *Int. J. Nav. Archit. Ocean Eng.*, **4** (2), 112-122. https://doi.org/10.2478/IJNAOE-2013-0082.

Ni, Y.Q., Hua, X.G., Fan, K.Q. and Ko, J.M. (2005), "Correlating modal properties with temperature using long-term monitoring data and support vector machine technique", *Eng. Struct.*, **27**(12), 1762-1773. https://doi.org/10.1016/j.engstruct.2005.02.020.

Packwood, A.R. (2000), "Flow through porous fences in thick boundary layers: comparisons between laboratory and numerical experiments", *J Wind Eng. Ind. Aerod.*, **88**(1), 75-90. https://doi.org/10.1016/S0167-6105(00)00025-8.

Papesch, A.J.G. (1992), "Wind tunnel test to optimize barrier spacing and porosity to reduce wind damage in horticultural shelter systems", *J. Wind Eng. Ind. Aerod.*, **44**(1-3), 2631-2642. https://doi.org/10.1016/0167-6105(92)90055-F.

Perera, M.D.A.E.S. (1981), "Shelter behind two-dimensional solid and porous fences", *J. Wind Eng. Ind. Aerod.*, **8**(1-2), 93-104. https://doi.org/10.1016/0167-6105(81)90010-6.

Purthviraj, U, Janardhan, P., Yaragal, S.C. and Nagaraj M.K., (2011), "Study on shelter effect of solid wind fences", *Int. J. Earth.Sci. Eng.*, **4**(01), 158-164.

Raine, J. K., and Stevenson, D. C. (1977), "Wind protection by model fences in a simulated atmospheric boundary layer", *J Wind Eng. Ind. Aerod.*, **2**(2), 159-180. https://doi.org/10.1016/0167-6105(77)90015-0.

Sagrado, A.P.G., van Beeck, J., Rambaud, P. and Olivari, D. (2002), "Numerical and experimental modelling of pollutant dispersion in a street canyon", *J. Wnd Eng. Ind. Aerod.*, **90**(4-5), 321-339. https://doi.org/10.1016/S0167-6105(01)00215-X.

Samui, P. (2008), "Predicted ultimate capacity of laterally loaded piles in clay using support vector machine", *Geomech. Geoeng.*, **3**(2), 113-120. https://doi.org/10.1080/17486020802050844.

San, B., Wang, Y. and Qiu, Y. (2018), "Numerical simulation and optimization study of the wind flow through a porous fence", *Environ. Fluid Mech.*, **18**(5), 1057-1075.

Santiago, J.L., Martin, F., Cuerva, A., Bezdenejnykh, N. and Sanz-Andres, A. (2007), "Experimental and numerical study of wind flow behind windbreaks", *Atmos. Environ.*, **41**(30), 6406-6420. https://doi.org/10.1016/j.atmosenv.2007.01.014.

Song, C.K., Kim, J.J. and Song, D.W. (2007), "The effects of windbreaks on reduction of suspended particles", *Atmosphere*, **17**(4), 315-326.

Středová, H., Podhrázská, J., Litschmann, T., Středa, T. and Rožnovský, J. (2012), "Aerodynamic parameters of windbreak based on its optical porosity", *Contributions to Geophysics and Geodesy*, **42**(3), 213-226.

Tani, N. (1958), "On the wind tunnel test of the model shelter hedge", *Bull. Natl. Inst. Agrid. Sci.*, Ser. **A 6**, 75.

Van Maele, K. and Merci, B. (2006), “Application of two buoyancy-modified k–ε turbulence models to different types of buoyant plumes”, *Fire Safety J.*, **41**(2), 122-138. https://doi.org/10.1016/j.firesaf.2005.11.003.
Vapnik, V. (1998), “Statistical Learning Theory”, Vol. 3, Wiley, New York.
Vapnik, V. (2013), “The Nature of Statistical Learning Theory”, Springer science & business media, New York, NY, USA
Vapnik, V.N. (1999), “An overview of statistical learning theory”, *IEEE T. Neural Networ.*, **10**(5).
Vapnik, V.N., Golowich, S.E. and Smola, A.J. (1996), “Support vector machine for function approximation, regression estimation, and signal processing”, *Adv. Neural Inf. Process*, **9**, 281-287.
Xu, Y. and Mustafa, M.Y. (2015), “Investigation of the structure of airflow behind a porous fence aided by CFD based virtual sensor data”, *Sensors & Transducers*, **185**(2), 149.
Yang, M.H., Roth, D. and Ahuja, N. (2002), “A tale of two classifiers: SNoW vs. SVM in visual recognition”, European Conference on Computer Vision, Springer, Berlin, Heidelberg, May, 685-699.
You, J., Jeon, J., You, K. and Kim, Y. (2006), “Experiment of the shelter effect of porous wind fences base on the wind tunnel test”, *Proceedings of the 2006 Architectural Institute of Korea*, **26**(1), 81-84.

CC